

Wave Measuring Buoy

Julian Beck, Oksana Wannick (Hochschule Bremerhaven)

Fachrichtung: Maritime Technologien, Studienphase: Bachelor, contact: oksana2.wannick@gmail.com

Wave measuring buoys are essential devices in ocean engineering. This article describes the process of designing a program that calculates useful wave parameters from measured raw acceleration data. The calculations are based on the assumption that the buoy analogue to a water particle travels on a circular orbit. The final program calculated position from the acceleration data and eliminated unwanted rotation of the coordinate system of the buoy. In a first field test the program turned out to be successful.

Key words: wave-measuring buoy, acceleration sensor, gyroscope, Matlab, rotating coordinate system, significant wave height.

1 Introduction

Ocean waves can be seen as influential economic factor for tourism, as well as for engineering and energy conversion. Water waves are appreciated for their beauty and feared for their destroying impact. Nowadays several alternative adapted technologies have been developed to measure wave data – however, wave measurements with help of buoys are still in use and will play a role in the future.

From March to July 2016 a wave measurement buoy project was conducted. It focused on an existing measurement buoy that was to follow the ocean surface motion and deliver acceleration, rotation and time data. Two previous student groups working on the project had already developed the basic hardware of the buoy. By combining and processing the data, the aim was to retrace the accelerations to motions and calculate characteristic wave parameters. For a better evaluation of the results of the processing, a second program was developed to simulate wave data. After a field test real waves could be analysed.

2 Theory of water waves

Basically, water waves are oscillating elevations of the ocean surface. If only one point is observed during a certain time, it gets obvious that in the time domain, water waves in their simplest appearance can be represented by sinusoidal oscillation. Observing points at several locations, at only one point of time, leads to the same result.

Water waves can be characterized by different parameters.

- One single wave is defined as the distance between two downward or two upward zero crossings in a time record. The temporal difference between them is called wave period T .¹
- The spatial difference between two successive peaks or troughs is defined as wave length λ .²

¹ Holthuijsen, 2007, p.26.



- The vertical distance between peak and trough of a wave is the wave height H .³

It is obvious that in reality one would not find this idealized wave shape with constant H , λ and T . These parameters vary statistically and waves with different parameters are overlain – commonly called sea state. **This is true for wave observations in general.** A wave measuring buoy works according to the following principle:

Focusing on a fixed point, like a water particle or even an idealized buoy, one will notice that it travels along a circular orbit during one wave period. The diameter of this orbit depends on the water depth. It is zero at the bottom and reaches a maximum at the sea surface.⁴ Furthermore, the orbital movement depends on the previously mentioned parameters.

The linear wave theory offers a connection between these parameters and the appearance of the orbital movement.⁵ This theory was the base for calculating test data for the buoy in order to be able to establish a processing routine before the first actual field-test.

3 Appearance and components of the buoy

The project focused on establishing a data processing routine for an existing buoy, whose hardware components – including the sensors – had been designed by two previous groups. Hence, in the following only the most important aspects shall be brought up.

The buoy is made up of a former deep-sea buoy, with a plastic housing containing a glass sphere. The sphere is equipped with a 3D acceleration sensor and a magnetometer (LSM303D)⁶, a gyroscope (L3GD20H)⁷ and a real time clock, supplied by batteries. Via a microcontroller the data is written onto a memory card. The frequency of measurement is 10 Hz. In order to ensure the free movement of the buoy, an additional anchoring buoy was applied to which the actual measuring buoy was connected via flexible mooring lines.

4 Methods: Data processing

In the following, the methods of the entire data processing will be presented. This includes the steps from the raw data that could be read from the memory card, centering and motion corrections and finally to calculating relevant parameters from the edited raw data and visualizing the results.

² Wright, Colling, Park, 1999, p.11.

³ Holthuijsen, 2007, p.27.

⁴ Ibid, p.121 ff.

⁵ Malcherek, 2010, p. 129 ff.

⁶ LSM303D – Datasheet, 2012, p.1.

⁷ L3GD20H - Datasheet, 2013, p.1.



4.1 Computer Program

To process the given data, the calculation program Matlab⁸ was chosen. The input data and equation systems can be seen as matrixes and can therefore be processed well since Matlab works matrix based. It provides helpful functions and toolboxes, specified more detailed below, and graphical user interfaces that were used to make the program user-friendly.⁹

4.2 Input Data

The given sensors measure data with a frequency of 10Hz, which is written on the SD-card as ASCII-files (American Standard Code for Information Interchange), thus simple text files. Every 30 minutes a new file is created. The data is written in rows of ten columns, which are: time (hours, minutes, seconds), acceleration (3D), gyroscope (3D), magnetometer (3D) (fig. 1).

1	22	29	27	2096	544	15568	39	-477	-51	-35	-262	-265
2	22	29	27	1696	592	15696	55	-443	-47	-34	-262	-265
3	22	29	27	1664	400	15712	48	-455	-45	-33	-259	-262
4	22	29	28	1568	528	15776	20	-504	-49	-33	-265	-266
5	22	29	28	1584	336	15680	16	-460	-39	-33	-265	-266
6	22	29	28	1680	336	15728	56	-450	-37	-32	-262	-267
7	22	29	28	1680	304	15728	67	-434	-39	-33	-264	-268
8	22	29	28	1728	320	15712	60	-426	-45	-34	-262	-267

Fig. 1: Raw data delivered by the sensor as ASCII-files. Columns l. to r.: time (hh), time (mm), time (ss), acceleration (x-axis), acceleration (y-axis), acceleration (z-axis), gyroscope (x-axis), gyroscope (y-axis), gyroscope (z-axis), magnetometer (x-axis, y-axis, z-axis).

As during the determined project time the magnetometer could not be included in the processing and the focus was on the acceleration data, the magnetometer data is not referred to in the following report.

The acceleration and gyroscope data are delivered in bits and saved as integers. To transform the data into m/s^2 and rad/s they can be multiplied by factors given in the datasheets. These are: $0.061\text{mg/LSB} = 5.9841 \cdot 10^{-4}(\text{m/s}^2)(1/\text{LSB})$ for the acceleration sensor¹⁰ and $8.75(\text{m}^\circ/\text{s})(1/\text{digit}) = 0.1527 \cdot 10^{-3}(\text{rad/s})(1/\text{digit})$.¹¹

In the following, the measured data columns are seen as numerical functions of time. They are expected to consist of oscillating functions (sine or cosine) because waves shall be measured that are oscillating themselves. However, the actual function is unknown.

⁸ MATLAB, Release 2016a.

⁹ Angermann, Beuschel, Rau, Wolfarth, 2011, S.1.

¹⁰ LSM303D – Datasheet, June 2012, p.10.

¹¹ L3GD20H - Datasheet, March 2013, p.10.



4.3 Calibration

Due to the sensors deviation, the measured data has to be calibrated to reduce measurement uncertainties by comparing measured values (V_m) to known values. As the sensors work linearly¹² in our range of measurement the data must only be calibrated by an offset (O) and multiplied by a factor (F). Therefore, a linear calibration with two known values per dataset is sufficient. The main idea for these known values was to choose values that can easily be measured manually and for which no extra equipment is needed. Therefore, the values for the calibration of the acceleration sensor are the positive and negative gravitational acceleration ($V_{k,acc} = \pm 9,81 \frac{m}{s^2}$), that can be measured simply by holding an axis vertical to the ground. Measuring an angular velocity to calibrate the gyroscope's axes is not possible manually, because a constant velocity will not be achieved. Therefore, the values for the calibration of the gyroscope are angles, which can be calculated by integration over time (t). The chosen values are $V_{k,gyr} = \pm 180^\circ$. These are measurable by a rotation around an axis.

For a linear calibration two equations must be solved. Each equation is equal to equation 1 or equation 2, depending on the sensor.

$$\text{Acceleration: } V_{k,acc} = V_{m,acc} \cdot F_{acc} + O_{acc} \quad (1)$$

$$\text{Gyroscope: } V_{k,gyr} = \int (V_{m,gyr} \cdot F_{gyr} + O_{gyr}) \cdot dt \quad (2a)$$

$$\Rightarrow V_{k,gyr} = (\int V_{m,gyr} \cdot dt) \cdot F_{gyr} + O_{gyr} \cdot \Delta t \quad (2b)$$

With these equations the offset and the factor can be calculated and eliminated by equation 3. The calibrated data (D_c) can be calculated out of the measured data (D_m). This is graphically shown in Fig. 2.

$$D_{c,acc} = D_{m,acc} \cdot F_{acc} + O_{acc} \quad (3a)$$

$$D_{c,gyr} = D_{m,gyr} \cdot F_{gyr} + O_{gyr} \quad (3b)$$

The offset and factor can differ for every measurement because they do not only depend on the kind of sensor but also on its age and environmental influences, e.g. temperature. Therefore, the calibration must be repeated for every new measurement.

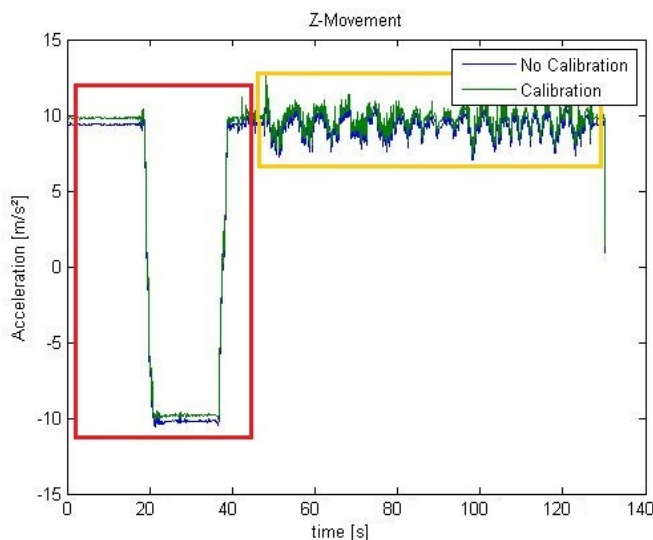


Fig.2: Example measurement of the acceleration sensor's z-axis. Blue curve: data that is not calibrated. Green curve: calibrated data. Red: calibration measurement. Orange: wave measurement.



4.4 Transformation and Integrations

The general idea for the processing was to integrate the accelerations (a) twice over time (t) to generate the velocity (v) and the distance (s) and therefore a 3D-movement of the buoy. From the vertical movement the wave heights can then be calculated. The general equation for the integration is equation 4, which is used for fixed coordinate systems.

$$a = \int v \cdot dt = \iint s \cdot dt \cdot dt \quad (4)$$

As the buoy rotates, the sensors' coordinate system is also rotating. This rotating coordinate system must firstly be transformed into a fixed coordinate system. The rotation matrix in equation 5 transfers a vector into a new coordinate system that can be rotated in three dimensions.

$$R_{\hat{n}}(\alpha) = \begin{pmatrix} n_1^2(1 - \cos \alpha) + \cos \alpha & n_1 n_2(1 - \cos \alpha) - n_3 \sin \alpha & n_1 n_3(1 - \cos \alpha) + n_2 \sin \alpha \\ n_2 n_1(1 - \cos \alpha) + n_3 \sin \alpha & n_2^2(1 - \cos \alpha) + \cos \alpha & n_2 n_3(1 - \cos \alpha) - n_1 \sin \alpha \\ n_3 n_1(1 - \cos \alpha) - n_2 \sin \alpha & n_3 n_2(1 - \cos \alpha) + n_1 \sin \alpha & n_3^2(1 - \cos \alpha) + \cos \alpha \end{pmatrix} \quad (5)^{13}$$

The angle α is the length of the angle vector $(\alpha_x, \alpha_y, \alpha_z)$ (eq. 6):

$$\alpha = \sqrt{\alpha_x^2 + \alpha_y^2 + \alpha_z^2} \quad (6) \text{ The unit vector}$$

\hat{n} is defined as shown in equation 7:

$$\hat{n} = \frac{(\alpha_x, \alpha_y, \alpha_z)}{\alpha} \quad (7)$$

To solve equation 5 the angle vector is needed (eq. 6, eq. 7). As the gyroscope measures an angular velocity in three dimensions, it is used to calculate a rotation angle (α) by integration over time (t) of the angle velocities (ω) (equation 8).

$$\alpha = \int \omega \cdot dt \quad (8)$$

If the integration is done from the beginning, the 3D rotation compared to the first measurement can be calculated for every state. The direction of the first coordinate system can then be seen as the fixed one. Therefore, the direction of the axis in the first measurement must be known and the z-axis should be vertical to the ground, because the height is calculated by the z-axis-data of the acceleration sensor.

After the data is transferred into one coordinate system, the accelerations can be integrated twice. All integrations must be done numerically, as we measure discrete data. We used the trapezoidal rule¹⁴ to calculate the numerical integral (Matlab function "cumtrapz"¹⁵). Equation 9 and 10 show the equation for the integration over time (t) with the trapezoidal rule for the angular velocity (eq. 9) and the distance (eq.10). Δt is given with 0.1s as we measure with a frequency of 10Hz. Two measurements are 0.1s apart from each other.

¹³ Baker.

¹⁴ Knorrenschild, 2013, p.121

¹⁵ MATLAB and Signal Processing Toolbox, Release 2014a.



$$\text{Analytical integration: } \omega = \int_{i=0}^N \alpha(t) \cdot dt \quad (9a)$$

$$\text{Numerical integration: } \omega = \sum_{i=0}^N \left(\frac{\alpha(t_i) + \alpha(t_i + \Delta t)}{2} \cdot \Delta t \right) \quad (9b)$$

$$\text{Analytical integration: } s = \int_{i=0}^N \int_{i=0}^N a \cdot dt dt \quad (10a)$$

$$\text{Numerical integration: } v = \sum_{i=0}^N \left(\frac{a(t_i) + a(t_i + \Delta t)}{2} \cdot \Delta t \right) \quad (10b)$$

$$s = \sum_{i=0}^N \left(\frac{v(t_i) + v(t_i + \Delta t)}{2} \cdot \Delta t \right) \quad (10c)$$

4.5 Polynomial Fit

A polynomial fit is also needed because a possible offset in the original function can lead into a linear offset in the first integration and a quadratic offset in the second integration (eq. 11).

$$\int (f(t) + O_1) dt = \int f(t) dt + O_1 \cdot t + O_2 \quad (11a)$$

$$\int \int (f(t) + O_1) dt dt =$$

$$\int \int f(t) dt dt + O_1 \cdot t^2 + O_2 \cdot t + O_3 \quad (11b)$$

The angle functions are fitted with a linear polynomial fit before transformation, while the distance functions are fitted with a quadratic polynomial fit. Matlab includes different helpful functions to do a polynomial fit (e.g. “polyfit”¹⁶ to calculate the coefficients to fit the given function and “polyval”¹⁷ to subtract the offset function). These were used instead of implementing an own function. Figure 3 shows the effect of a polynomial fit.

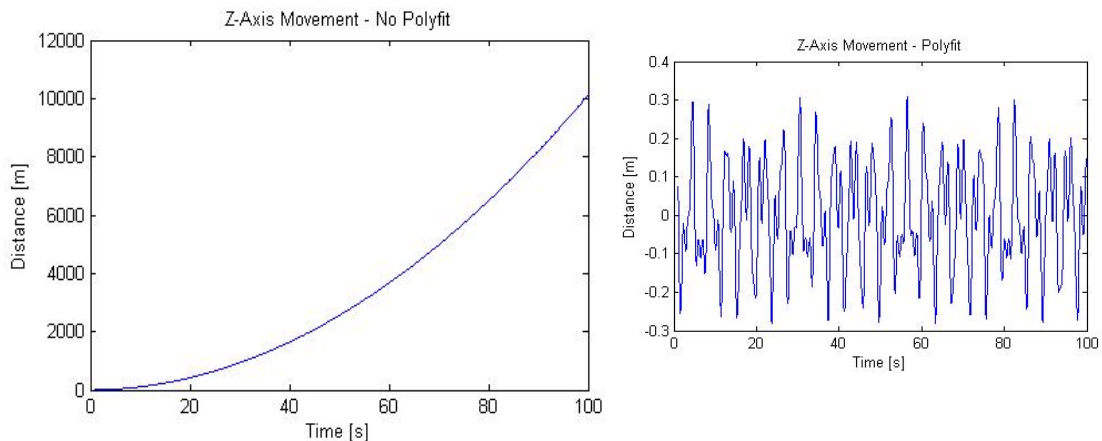


Fig.3: Example data of the acceleration sensor's z-axis after transformation and double integration. Left: data that is not polyfitted and overlain by a quadratic function ($f(t)+O \cdot t^2$). Right: data that is polyfitted. Quadratic error function is reduced ($f(t)$)

¹⁶ MATLAB and Signal Processing Toolbox, Release 2014a.

¹⁷ MATLAB and Signal Processing Toolbox, Release 2014a.



4.6 Filtering

Filtering the calculated data is important, because after the calibration and transformation the measurement can still be overlain by noise. These can be oscillations with very high, but also very low frequencies. As we integrate our measurements, mainly oscillations with low frequencies have a high impact on the measurement. Equation 12 depicts that the original oscillation with the amplitude A is divided by the frequency (f) when integrated. Therefore the error due to low frequent oscillations is dominant.

$$\int A \cdot \cos(2\pi f \cdot t) dt = \frac{1}{2\pi f} \cdot A \cdot \sin(2\pi f \cdot t) \quad (12)$$

As the buoy's hardware already existed and the sensors deliver digital data, an analogue filter was not possible. Therefore, a digital filter was implemented. A second order butterworth band pass filter was the filter of choice. A band pass filter is needed because low and high noise frequencies shall be cut off. A butterworth filter is useful because it has the flattest frequency respond in the pass band and the passing frequencies shall not be changed. The slower roll-off compared to other filters is no problem because the low error frequencies and the needed wave frequencies are fading into each other and therefore a perfect cut off frequency cannot be found. The butterworth filter is implemented into Matlab with the help of the "Signal Processing Toolbox" and the functions "butter" and "filtfilt".¹⁸ The cut off frequencies were found empirically by measuring known movements and comparing them to the processed data with different filter coefficients. The gained coefficients are shown in table 1. The angle functions are filtered before the transformation, the distance functions are filtered after the polynomial fit. Figure 4 on the following page shows an example measurement with and without the digital filter.

	Acceleration sensor	Gyroscope
Low cut off frequency	0.3 Hz	0.05 Hz
High cut off frequency	2 Hz	3 Hz

Table 1: Empirically chosen cut off frequencies for the different sensors, for a second order butterworth band pass filter.

¹⁸ MATLAB and Signal Processing Toolbox, Release 2014a.



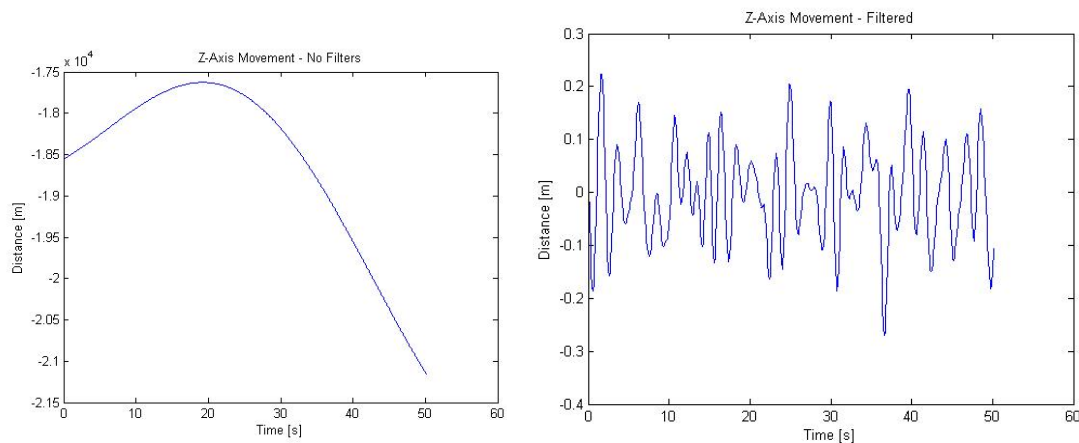


Fig.4: Example data of the acceleration sensor's z-axis after transformation, double integration and polyfit. Left: data processed without any filters. Right: data processed with all filters included. The waves are also present in the upper graph, but they are too small to be seen besides the dominant noise.

4.7 Wave Parameters

Significant wave height

The most influential parameter in coastal engineering is the significant wave height, defined as the mean of the highest third of waves in the wave record¹⁹, $H_{1/3}$. This definition results from visual observation where the smaller waves tend to be neglected. An easily implemented method to find $H_{1/3}$ is to calculate the mean of the absolute highest third of wave height data in a time series. This method turned out to be efficient in tests. However, this point of view suggests that each wave produces the same amount of data, which means that the wave periods have to be roughly the same. A second, scientifically more correct approach is to split the entirely measured data in subdivisions of 30 minutes and using the Matlab Signal Processing Toolbox detecting the turning points by a built-in function.²⁰ These are the true wave peaks. The highest third of these values is averaged as in the first process.

After all, there was no considerable difference between the results that the two routines delivered. Nevertheless, due to the implementation by definition the second approach was used for the final processing.

Significant wave period

According to the significant wave height, the significant wave period is the mean period of the highest one third of waves²¹, $T_{1/3}$. A first idea was to calculate it consistently with the significant wave height, meaning to eliminate all wave heights below and to calculate the

¹⁹ Holthuijsen, 2007, p.28.

²⁰ MATLAB and Signal Processing Toolbox, Release 2014a.

²¹ Ibid, p.29.



delay between two remaining upward zero crossings, as figure 5 suggests. Since the appearance of the waves varied so strongly from case to case and that in most cases after the first step an insufficient amount of data persisted, this method lead to no trustworthy results.

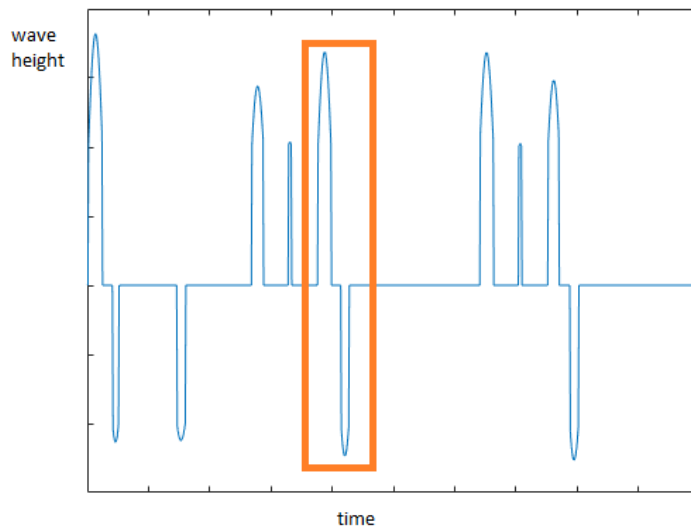


Fig.5: Only considering the wave heights above the significant wave height and measuring the distances between two upward zero crossings. One example wave period is marked.

As an alternative, a second approach was via Fourier frequency analysis. The results were more reliable and due to built-in Matlab functions the calculation was less complex. This was then the method of choice.

Wave length

As the buoy is dealt with as one single point in the model used for the calculations, the wavelength λ cannot be measured directly.

It can be calculated, though, when the wave period T is known.²²

$$\lambda = \frac{gT^2}{2\pi} \quad (13)$$

Where g is the acceleration due to earth gravity.

This makes it easy to implement the calculation, but it means also that the quality of the result depends on the accuracy of the wave period. Furthermore, it has to be considered that the previously calculated wave period is not an absolute one, but based on the highest third of the waves. One could also speak of a significant wavelength, although this is no technical term.

From these three parameters, as necessary, further wave characteristics like wave speed or average energy content can be calculated.

²² Wright et al., 1999, p.11.



4.8 Field Measurement

From May 30, 2016, 9:16am to June, 1, 2016, 8:50am the wave measuring buoy was installed in the research area of the Lysekil Wave Power Project from Uppsala, at the west coast of Sweden, close to Lysekil.²³ This took place during the “Third workshop for marine energy at Sven Lovén Centre”.²⁴

The buoy measured data during the whole time period. A calibration measurement was done on May 29. In the research area a Datawell Waverider wave-measuring buoy was installed since 2004.²⁵ The data of the two buoys were compared (fig. 6). In the final chapter we focus on the comparison of May 31, as data was measured the whole day.

4.9 Comparison – field test and reference data

One can see that the significant wave heights measured and processed by us is lower than the data from the Datawell Waverider (fig.6). Still the relative trend of the curves is identical. Between 0:00 and 5:00 the wave height fluctuates at about 0.15 m. Then the curve rises until a peak at 9:00/9:30. A low point of 0.1m can be seen in both curves at 10:30, followed by a fluctuation around 0.2m from 11:00 to 18:00. Still our calculated wave height stays 0.05 m to 0.1 m lower than the reference data. From 19:30 to 23:30 both graphs show a wave height of around 0.1 m.

²³ Leijon et al., 2008, p.221.

²⁴ Bochert and Remouit (ed.), 2016, p.5.

²⁵ Leijon et al., 2008, p.225.



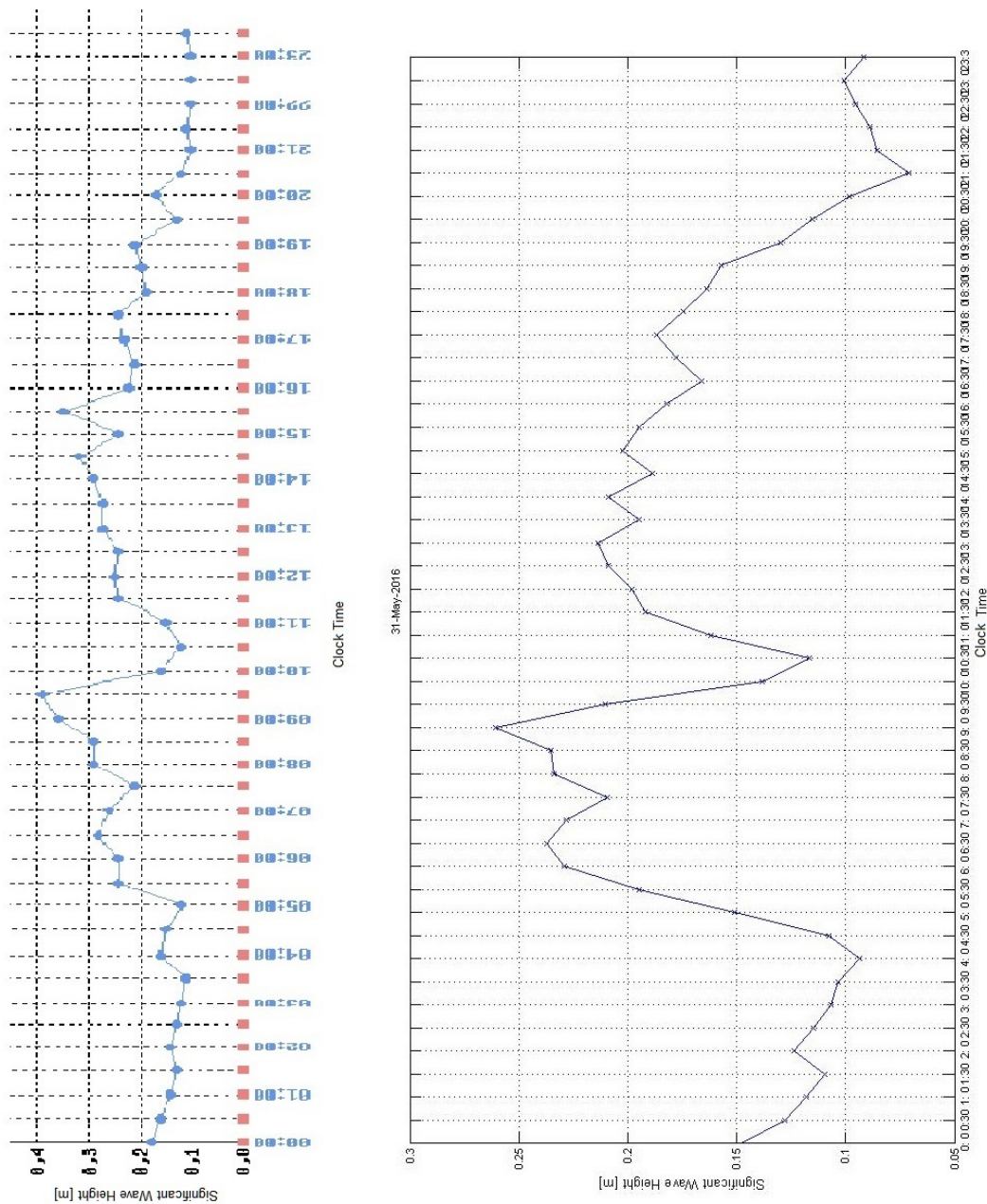


Fig.6: Comparison of the data measured by our wave-measuring buoy (left) and the Datawell Waverider wave-measuring buoy (right) installed at the Lysekil research area. Date: 31st May. X-axis: Time, Y-axis: significant wave height.

5 Possible sources of error

Although the field test turned out to be successful, several sources of error could be detected that affect the accuracy of the results or that could have been optimized or handled differently during the development process.



5.1 Development process of the program

As previously mentioned, the final program was developed based on simulated data before the actual field test. This means that inaccuracies and errors in the simulation could have led to further errors.

Moreover, the entire methodology of the calculation is based on numerical methods.

According to the sampling theorem by Shannon and Kotelnikov, the sampling frequency has to be higher than twice the highest frequency of the signal²⁶:

$$f_a > 2f_h \quad (14)$$

The sampling frequency in the measurement is 10 Hz, which is far higher than the highest expected frequency. This frequency is, referring to W. H. Munk, 1 Hz.²⁷ Therefore, the error of using numerical functions can almost be neglected.

5.2 Calculation of significant wave height

There is no standardized definition of the significant wave height. The above formula depicts the result that comparable observations and estimations would have led to.²⁸ This means that the significant wave height is no absolutely accurate value, but rather stands for a possible wave height interval.

When any other parameter, for example the average energy content of a wave, is calculated with help of $H_{1/3}$, this has to be kept in mind.

5.3 General errors with buoy measurements

The above-mentioned aspects explain how the measurement of the buoy could have been influenced. So far, it has been completely neglected that the constitution of a buoy cannot completely represent the real wave climate. As the buoy is not simply a point, but has a volume and a mass, small waves tend to be neglected. Additionally, the measured data compared with the actual wave tend to look more symmetrical, crests are sharper and troughs flatter in reality.²⁹ If they are known, for example because of reference measurements by other instruments, these errors could be eliminated. Since the only reference in the field test was another buoy, this was not possible.

²⁶ Hoffmann (ed.), 2011, p.129.

²⁷ Munk, 1950, p.1.

²⁸ Malcherek, 2010, p. 191.

²⁹ Holthuijsen, 2007, S.13.



5.4 Accuracy of the sensor

According to the data sheet the acceleration measurement has a sensitivity of 0.061 mg/LSB and the magnetic measurement one of 0.080 mGauss/LSB.³⁰

Thus, these values lose their significance during the processing. After the filtering and the polynomial fit it cannot be generally retraced with which factor these accuracies influence the resulting distances.

6 Conclusion and Outlook

The wave-measuring buoy and our processing program work very well, but are not as accurate as professional wave measuring buoys. Also, with 0.1m to 0.4m, only a small range of significant wave heights was measured, leading to a lack of comparability.

In spite, comparing the methods and the financial aspects, especially for the sensor, compared with relatively expensive commercial buoys, an effective alternative was found.

The project can be improved by further field tests in different wave climates and adaptations of filter coefficients. The magnetometer, which delivers further information and could be included to improve the performance, is also not included. Changing the Butterworth to a Kalman filter or doing automatic calibrations during the measurement could include it.

7 References

- Angermann, A., Beuschel, M., Rau, M. Wolfarth, U. (2011). Matlab – Simulink – Stateflow. München: Oldenbourg.
- Baker, M. J. (o.D.). Maths – Axis Angle to Matrix. Abgerufen am 21.08.2016: <http://www.euclideanspace.com/maths/geometry/rotations/conversions/angleToMatrix/>.
- Bochert, A. and Remouit, F. (Ed.). (2016). Proceedings of the Third Workshop for Marine Energy at the Sven Lovén Centre. Bremerhaven and Uppsala.
- Hoffmann, J. (Ed.). (2011). Taschenbuch der Messtechnik. München: Carl Hanser Verlag.
- Holthuijsen, L. H. (2007). Waves in oceanic and coastal waters. Cambridge: Cambridge University Press.
- Knorrenschild, M. (2013). Numerische Mathematik. Leipzig: Carl Hanser Verlag GmbH & Co. KG.
- Leijon, M., Boström, C., Danielsson, O., Gustafsson, S., Haikonen, K., Langhammer, O., et al. (2008). Wave Energy from the North Sea: Experiences from the Lysekil Research Site. (Springerlink.com). Surv Geophys. (S.221-240). Abgerufen am 21.08.2016: <http://link.springer.com/article/10.1007%2F978-90-47-9047-x>.

³⁰ LSM303D – Datasheet, June 2012, p.10.



LSM303D – Datasheet, (2012). STMicroelectronics. Abgerufen von: https://www.pololu.com/file/download/LSM303D.pdf?file_id=0J703.

L3GD20H – Datasheet, (2013). STMicroelectronics. Abgerufen von: <https://www.pololu.com/file/0J731/L3GD20H.pdf>.

Malcherek, A. (2010). Gezeiten und Wellen – Die Hydromechanik der Küstengewässer. Wiesbaden: Vieweg+ Teubner.

MATLAB. (Release 2016a). The MathWorks, Inc., Natick.

MATLAB and Signal Processing Toolbox. (Release 2014a). The MathWorks, Inc., Natick.

Munk, W. H. (1950). Origin and generation of waves. La Jolla.

Wright, J., Colling, A., & Park, D. (1999). Waves, tides, and shallow-water processes (Vol. 4). Milton Keynes: The Open University.

